Joint Image Denoising and Demosaicking by Low Rank Approximation and Color Difference Model

Xia Zhai[1], Weiwei Guo[2], Yongqin Zhang[3], Jinsheng Xiao[4], and Xiaoguang Hu[5]
[1]Arts Department, Henan University of Economics and Law, China
[2]Department of Information and Communication Engineering, University of Electronic Science and Technology, China
[3]School of Information Science and Technology, Northwest University, China
[4]School of Electronic Information, Wuhan University, China
[5]School of Criminal Science and Technology, People's Public Security University of China, China

Abstract: *Digital cameras generally use a single image sensor which surface is covered by a color filter array. The Color Filter Array* (*CFA*) *limits each sensor pixel by sampling one of the three primary color values (red, green or blue), whereas the other two missing color values would be acquired by the post-processing procedure called demosaicking. From the noisy CFA data, the full color images are reconstructed through an imaging pipeline of demosaicking and denoising. However, image denoising in the RGB space has expensive computation cost. In this paper, to increase the efficiency and the color fidelity, we propose a novel joint denoising and demosaicking strategy to reconstruct the noiseless full color image from the input noisy CFA data. The low-rank approximation technique is first used to remove the noise from CFA data. Then, image demosaicking using both color difference space and signal correlation are applied to the denoised CFA data to obtain the noise-less full color image. The experimental results show that the proposed algorithm not only improves the quality of full color image but also outperforms the existing state-of-the-art methods both subjectively and objectively.*

Keywords: *Image denoising, image demosaicking, CFA, low rank approximation, color difference model.*

Received May 8, 2013; accepted June 1, 2014

1. Introduction

The digital cameras are important imaging equipment for image processing and computer vision. The full color digital images are usually composed of three different spectral components, i.e., red, green and blue. It is desirable of having three Complementary Metal Oxide Semiconductor (CMOS)/Charge Coupled Device (CCD) image sensors to capture full color digital images. However, in order to decrease the production cost, most digital color cameras only use a single sensor with only one Color Filter Array (CFA) instead of three. Therefore, the color interpolation or demosaicking is applied to the CFA data to reconstruct the full color images. Generally speaking, image denoising is carried out after image demosaicking in many applications. In the real world, the noise of digital cameras mainly comes from electrical components. The pixel sensor of the CMOS devices typically consists of a photodiode and three transistors, which are the major sources of noise. Consequently, image denoising is an essential preprocessing step to reconstruct the full color image. In recent decades, many image denoising methods have appeared and received considerable attention, such as wavelet-based methods [8], the bilateral filtering [9], the non-local means [2], the low rank technique [15] and the others [1, 10, 14]. However, these methods did not consider that image demosaicking has the amplification effects of noise in CFA data, which caused the blurred edges and smoothed textures of the output images.

Image demosaicking plays a very important role to generate full color images. So far, great progress has been made in theoretical research of image demosaicking and many methods have been introduced into the studies. They can be mainly divided into two categories. One is directly to interpolate each color channel separately, which produces good results when applied to gray-scale images. Unfortunately, when applied to color images, they often lead to visible color artifacts in the reconstructed images. The other is to interpolate through the signal correlation among the color channels [4, 6, 11], which has better performance in color fidelity. Recently, many demosaicking methods have been proposed. Gunturk *et al.* [4] exploited the inter-channel correlation in an alternating projection scheme, which outperforms the nearest-neighbor replication, bilinear interpolation and cubic spline interpolation. Yuk *et al.* [11] developed another demosaicking method that selects direction adaptively for interpolation using the direction similarity in different color spaces. However, these demosaicking methods often lead to color artifacts in reconstructed images. In fact, the acquired CFA data is generally noisy, which causes the interpolation error

and color distortion. However, most demosaicking methods are used to reconstruct the full color images on the assumption that the CFA data is noise-free.

In order to make the assumption more realistic, some researchers have put forward novel methods that generate the full color image from the noisy CFA signal [3, 5, 7, 12, 13, 16]. Hirakawa and Parks [5] proposed a joint of demosaicking and denoising algorithm. They treated both demosaicking and denoising as estimation problems, and proposed an optimal image filter based on the Total Least Square (TLS) technique. Zhang *et al.* [13] exploited both spectral and spatial correlations to suppress sensor noise and interpolation error simultaneously by using the Linear Minimum Mean Square-Error (LMMSE) technique. Menon and Calvagno [7] adopted the space-varying filters and the evaluation of noise autocorrelation to reconstruct the full resolution color image. Zhang *et al.* [12] developed a spatially adaptive method based on Principle Component Analysis (PCA), which worked on the noisy CFA data by supporting window to analyze the local image statistics. Condat and Mosaddegh [3] presented a joint demosaicking and denoising framework by total variation minimization to construct the full color image.

In this paper, we present a united denoising and demosaicking framework based on both the low rank approximation and color difference model. The proposed algorithm employs a low rank approximation strategy for the local patches to achieve resolution enhancement and noise removal. The low rank approximation adopts the refined parallel analysis with Monte Carlo simulation to select signal subspace dimensionality of the noisy patches. In order to obtain the full color image, the adaptive edge-preserving and edge-directed interpolation method is proposed for color reproduction from the denoised CFA data. Finally, according to the image observation model, the simulation results of the synthetic images with variant noise levels demonstrate that the proposed algorithm outperforms the state-of-the-art methods both quantitatively and qualitatively.

The remainder of this paper is organized as follows. In section 2, we briefly review the image observation model, and then describe the proposed algorithm in detail. Section 3 gives the experimental evaluations and comparisons. At last, section 4 draws the conclusions.

2. Proposed Algorithm

To produce high quality images acquired by digital cameras, many methods have been proposed to reconstruct the full color images. There are mainly three schemes to reconstruct the full color image from the noisy CFA data. One is demosaicking first and followed denoising, the second is joint demosaicking and denoising together, and the third is denoising first and demosaicking later. For the first scheme, it is still a challenging problem in image processing. The noise in CFA data will affect the demosaicked results and caused color artifacts, which is difficult to be removed in the following denoising processing. The first scheme also has the drawbacks of high computational cost. Consequently, the second and third schemes are generally used to derive the full color images. In this paper, we will only study the third scheme to build the full color images.

2.1. Image Observation Model

The mathematical model of the observed noisy images [5] is given as follows:

$$Y(i,j) = X(i,j) + \delta(k_0 + k_1 X(i,j)) \quad (1)$$

Where $x(i, j)$ and $y(i, j)$ are separately the ideal and measured sensor values at pixel location (i, j), $\delta \sim N(0,1)$ is the noise, k_0 and k_1 are sensor dependent parameters. Specifically, the noisy color images can be described in another formula [13]:

$$\tilde{r} = r + v_r, \quad \tilde{g} = g + v_g, \quad \tilde{b} = b + v_b \quad (2)$$

Where v_r, v_g and v_b are the noise in the red, green and blue channel, r, g and b are the ideal values, $\tilde{r}$, $\tilde{g}$ and $\tilde{b}$ are the noisy signals. In fact, the acquired images from the CCD/CMOS sensors often contain the additive and/or multiplicative noises. However, only noisy CFA image data is available in practice. In order to reconstruct the noiseless full color image, we propose the joint denoising and demosaicking algorithm that employs the low rank approximation and color difference model for the noisy CFA data. The proposed blind algorithm mainly consists of two steps: The CFA denoising and image demosaicking.

2.2. CFA Denoising Step

Different from the existing patch-based denoising methods, the proposed algorithm utilizes the projections of local patch stacks onto signal subspace. For each patch of the CFA data, the signal dimensionality was determined by the refined parallel analysis with Monte Carlo simulation. After the projection of each patch onto its signal subspace, the denoised CFA data is acquired by patch alignment and the averaging method.

First of all, the denoising step is implemented to remove noise of the noisy CFA data. Assume that $x(i, j)$ is the true pixel value at the spatial location (i, j) of the observed image $X \in R^{M \times N}$ and Y is a patch-based representation of X. Those $\sqrt{P} \times \sqrt{P}$ pixels around the center pixel $x(i, j)$ in the image X constitute a reshaped column vector from Y. That is to say, Y is a matrix of

size $M\times N\times P$, which consists of the pixels in the image X.

Suppose that, the image patch centered at $x(i, j)$ is in a $\sqrt{L}\times\sqrt{L}$ sliding search window. The image matrix X will be divided into $M_D\times N_D$ image blocks of the same size $\sqrt{D}\times\sqrt{D}$. To ensure that the search window covers all the related image blocks, we define $\sqrt{L}\,3\sqrt{D}+\sqrt{P}$ -1. For each image block, its similar patches are found by block matching method. Then these similar patches are reorganized as the matrix $Z_{m,n}$ with the size of $L\times P$, where m=1, …, M_D and n=1, …, N_D.

According to Singular Value Decomposition (SVD) of the similar patch group, the most energy of the image signal concentrates on the first few principal components, while the energy of noise will evenly spread over the whole components. Hence, the optimal dimensionality of PCA can be used for noise removal. By removing the mean value from each column vectors, the zero-centered image matrix is given as:

$$\overline{Z}_{m,n} = Z_{m,n}(\mathrm{l}, p) - \frac{1}{L}\sum_{l=1}^{L} Z_{m,n}(\mathrm{l}, p) \tag{3}$$

Where l=1, ..., L, p=1, ..., P, m=1, ..., M_D, n=1, …, N_D. To reduce the calculation time on the condition of $L>P$, we replace $\overline{Z}_{m,n}$ with the covariance matrix $\overline{Z}^{T}_{m,n}\overline{Z}_{m,n}$. Thus, we have:

$$\overline{Z}^{T}_{m,n}\overline{Z}_{m,n}U = U\,{}^{2}\,{}^{T} \tag{4}$$

Where U = [u_1, u_2, ..., u_p] is the $P\times P$ unitary matrix consisted of eigenvectors derived from $\overline{Z}^{T}_{m,n}\overline{Z}_{m,n}$. Define $\Sigma=diag\{\lambda_1, \lambda_2, \ldots, \lambda_p\}$ as the $P\times P$ diagonal matrix, $\lambda_1\geq\ldots\geq\lambda_r\geq 0$, $r = rank(\overline{Z}^{T}_{m,n}\overline{Z}_{m,n})$, where λ_1, …, λ_r are the singular values of $\overline{Z}^{T}_{m,n}\overline{Z}_{m,n}$. By this projection, $\overline{Z}^{T}_{m,n}\overline{Z}_{m,n}$ can be decorrelated, and $\overline{Z}_{m,n}$ is projected onto the basis U, the reformed uncorrelated matrix $\widehat{Z}_{m,n}$ is given as:

$$\widehat{Z}_{m,n} = \overline{Z}_{m,n}\times U \tag{5}$$

According to principle component analysis, we find that the images can be reconstructed only by several important components. The output images would not lose much information if the small singular values are ignored and the image patch size is large enough. Therefore, we can only use the first K eigenvectors to reconstruct the noiseless CFA data, which not only removes the noise but also preserves the most image information. In our algorithm, we adopt the refined parallel analysis with Monte Carlo simulation to select the signal components.

Let the singular values of the image patch $\overline{Z}_{m,n}$ be denoted by λ_p sorted in the descending order, where p=1, ..., P. Assume α_p as the singular values of the artificial data. So, the parallel analysis can estimate the signal dimensionality of noisy image data as follows:

$$K = max\{p \,\dot{\div}\, 1\alpha L, P\,\big|\,{}_{p}{}^{3}\;{}_{p}\} \tag{6}$$

Where α_p is a threshold and the singular value λ_p less than α_p is discarded to remove noise.

In order to estimate the signal subspace dimensionality from noisy image data, we generate the artificial data with the same size of the image patches. Let $C\in R^{L\times P}$ denote the artificial matrix. Similarly, we use C^TC instead of C for the projection of the artificial data. The SVD of this artificial data matrix is given as:

$$C^{T}C = VS^{2}V \tag{7}$$

Where V is the unitary matrix of eigenvectors derived from the artificial data matrix, and $S=diag\{\beta_1, \beta_2, \ldots, \beta_p\}$ is a diagonal matrix with its singular value in the descending order. Let β_p for p=1, ..., P denote the singular values of the artificial data matrix. Then we compare λ_p with β_p to determinate the signal subspace dimensionality:

$$K = max\{p \,\dot{\div}\, 1\beta L, P\,\big|\,{}_{p}{}^{3}\;{}_{p}\} \tag{8}$$

Through the refined parallel analysis, the signal subspace dimensionality is determined so that we can reconstruct the noiseless image. For each image block, the straight forward way to reconstruct a noiseless image block is to project the noisy column vectors directly onto the subspace of the first K eigenvectors in a low rank representation. Hence, each projected weight matrix of signal subspace is:

$$W_{m,n}(k, p) = \widehat{Z}_{m,n}(\mathrm{l}, k)\big/\overline{Z}_{m,n}(\mathrm{l}, p) \tag{9}$$

Where k=1, 2, …, K and p=1, 2, ..., P. Then, the noiseless image patch stack $R_{m,n}$ is acquired by the weighted subspace as follows:

$$R_{m,n} = \widehat{Z}_{m,n}(\mathrm{l}, k)W_{m,n}(k, p) + \frac{1}{L}Z_{m,n}(\mathrm{l}, p) \tag{10}$$

Finally, we can reconstruct the noiseless image F by patch alignment technique and overlap averaging scheme for the whole image. Each pixel value at the position (i, j) would be described by this formula:

$$F(i, j) = \frac{1}{n_x}\sum_{m,n,p}^{M_D,N_D,P} R_{m,n}(\mathrm{l}, p) \tag{11}$$

Where n_x is the number of pixels used in the image patch stacks for the whole image.

Our proposed denoising algorithm is used to reduce the noise of the CFA data in the blind condition. In order to reconstruct a full color image, the proposed interpolation step called demosaicking is performed on the denoised CFA data.

2.3. Image Demosaicking Step

Most consumer cameras capture images by a Bayer CFA pattern that only one color value is sampled at the location of each pixel. The Bayer pattern is shown in Figure 1, which provides an array of red (r), green (g) and blue (b) color components. Since, only a single color component is available at each spatial location, the demosaicking is used to interpolate the other two missing color components.

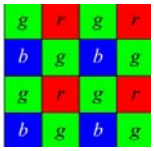

Figure 1. Bayer CFA pattern.

Yuk *et al.* [11] proposed a simple demosaicking method which interpolates in color difference space. In order to avoid interpolation across the edge and reduce color artifacts, it interpolates color images using the direction similarity. However, this method ignores that the adjacent pixels have different correlation along the different directions. To reduce color artifacts, another demosaicking method [16] exploits the adaptive spatial correlation to interpolate the pixels in the color difference space for the full color image reconstruction. In our algorithm, we employ the color difference model for image demosaicking due to its low contrast.

Assume that *R*, *G* and *B* are the desired image color values obtained by a digital camera, and *R'*, *G'* and *B'* are interpolated values. Their normalized values are between 0 and 1. We separately compute the differences between color channels, i.e., K_R (green minus red) and K_B (green minus blue), and then interpolated them. Thus, the full color image is reconstructed by the interpolation method.

Firstly, we describe how to compute K_R/K_B at the red/blue pixels. According to the structural similarity, the interpolation direction should be determined before the interpolation operation. Let *L*, *R*, *U* and *D* is the index of *R*, *G* and *B*. *H* and *V* denote the image's horizontal and vertical interpolation direction, respectively.

As is shown in Figure 2, we interpolate the pixel at the location *R*, the similarity between horizontal and vertical directions can be calculated as:

$$\begin{cases} V = \left|K_R - K_{R_{U2}}\right| + \left|K_R - K_{R_{D2}}\right| \\ H = \left|K_R - K_{R_{L2}}\right| + \left|K_R - K_{R_{R2}}\right| \end{cases} \quad (12)$$

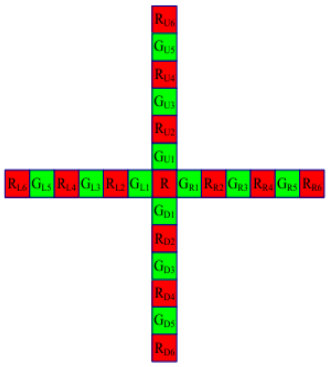

Figure 2. Interpolated K_R at the red pixel.

After computing the similarity between horizontal and vertical directions, we select the dominant direction for the interpolation. That is, if their values are comparatively different, the direction of interpolation is selected according to smoother direction. Otherwise, we should select a bigger window to determine the direction of interpolation. In our algorithm, if $|H-V| < c\ |H+V|$, then we will choose the bigger window and calculate *H* and *V* again as follows:

$$\begin{cases} V = \left|K_R - K_{R_{U2}}\right| + \left|K_{R_{U2}} - K_{R_{D2}}\right| + \left|K_R - K_{R_{D4}}\right| \\ H = \left|K_R - K_{R_{L4}}\right| + \left|K_{R_{L2}} - K_{R_{R2}}\right| + \left|K_R - K_{R_{R4}}\right| \end{cases} \quad (13)$$

If $H>V$, $K_R=0.5\ (G_{UI}+G_{DI})-0.25(R_{U2}+2R+R_{D2})$, otherwise, $K_R=0.5\ (G_{LI}+G_{RI})-0.25(R_{L2}+2R+R_{R2})$.

The estimation of K_B at *B* pixels is performed in the similar way. Next we compute K_R/K_B at the blue/red pixels. Here, we take the estimation of K_R for example. According to Figure 3, we compute K_R at *R* pixels with diagonal neighboring locations in the following form:

$$K_R = 0.25(K_{R1} + K_{R2} + K_{R3} + K_{R4}) \quad (14)$$

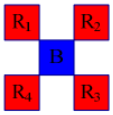

Figure 3. Interpolated K_R at the blue pixel.

Next, we compute K_R/K_B at the green pixels. Referring to Figure 4, since the interpolated K_R/K_B values at the blue/red pixels are available by the previous procedures, we calculate K_R/K_B at green pixels as the weighted sum of vertical and horizontal direction similarity. The process is approximately similar with the computation of K_R/K_B at red/blue pixels.

$$\begin{cases} V = 0.5\left|K_{R_{D1}} - K_{R_{U3}}\right| + 0.5\left|K_{R_{U1}} - K_{R_{D3}}\right| \\ H = 0.5\left|K_{R_{R1}} - K_{R_{L3}}\right| + 0.5\left|K_{R_{L1}} - K_{R_{R3}}\right| \end{cases} \quad (15)$$

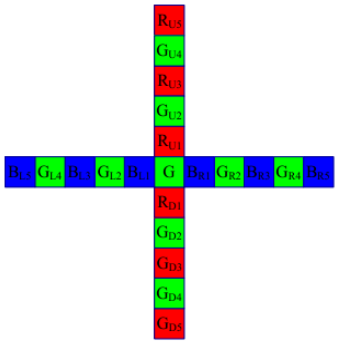

Figure 4. Interpolated K_R at the green pixel.

If $|H-V|<c\ |H+V|$, we choose a larger window and compute H and V again. Then, we have:

$$K_R = \begin{cases} 0.5(K_{R_{D1}} + K_{R_{U1}}), & H > V \\ 0.5(K_{R_{L1}} + K_{R_{R1}}), & others. \end{cases} \quad (16)$$

The same process is performed to compute K_B values at green pixels.

After all K_R/K_B are obtained at each pixel, we calculate the missing pixel values to generate the full color image. Finally, at R channel, the pixel value is:

$$R' = R,\ G' = R + K_R,\ B' = G' - K_B \quad (17)$$

At G channel, the pixel value is:

$$G' = G,\ R' = G - K_R,\ B' = G - K_B \quad (18)$$

At B channel, the pixel value is:

$$B' = B,\ G' = G + K_B,\ R' = G' - K_R \quad (19)$$

3. Simulation Results

To evaluate the performance of the proposed algorithm comprehensively, the experiments were carried out. A set of test images is selected from the well-known Kodak dataset. In our experiments, we compare our proposed algorithm with the PCA-based spatially adaptive denoising [12] and the joint demosaicing and denoising [5]. The performances of these different methods were evaluated on the test images by Peak Signal-To-Noise Ratio (PSNR) and Structural Similarity (SSIM).

In the experiment, the test color images were mosaicked with the Bayer CFA and corrupted by the speckle noise model with different deviations 0.0100, 0.0225 and 0.0400, respectively. The parameters of our proposed algorithm is set with the variable search window of 25×25 pixels, the image block of 17×17 pixels and the neighborhood patch of 7×7 pixels for noise removal. Moreover, the color demosaicking with adaptive window size is used to reconstruct the full color images from the CFA data. According to the similarity between horizontal and vertical directions, the demosaicking step adaptively selects one of three different windows of size 9×9, 13×13 and 17×17. Figure 5 shows the simulated noisy color images generated from 'kodim21' corrupted by the speckle noise with different deviations 0.0100, 0.0225 and 0.0400, respectively. The visual comparison of these different methods for the test image 'kodim21' is given in Figure 6. For a set of test Kodak color images, the PSNR(dB)/SSIM results are presented in Table 1. As can be seen from the results, the proposed algorithm has less color artifacts and sharper edges. The experimental results demonstrate that our proposed algorithm can suppress the noise and preserve the image details efficiently, and outperforms the state-of-the-art methods both objectively and subjectivel.

Figure 5. The test color image 'kodim21' corrupted by speckle noise with different deviations 0.0100, 0.0225 and 0.0400, respectively.

a) PCA [12].

b) TLS [5].

c) Our proposed algorithm.

Figure 6. The visual comparisons of the results obtained by [5, 13] and our proposed algorithm for the test image 'kodim21' corrupted by speckle noise with deviations 0.0100, 0.0225 and 0.0400, respectively. From left to right: the first row (a), the second row (b) and the last row (c) are separately the results obtained by [5, 13] and our proposed algorithm for the simulated noisy images in Figure 5.

Table 1. The comparison of PSNR(dB)/SSIM results obtained by these different methods.

PSNR/SSIM		TLS [5]			PCA [13]			Proposed		
		0.0100	0.0225	0.0400	0.0100	0.0225	0.0400	0.0100	0.0225	0.0400
kodim03	R	27.22/0.5754	24.21/0.4161	21.95/0.3106	29.73/0.6138	26.66/0.4602	25.09/0.3766	30.31/0.8467	29.22/0.7989	28.10/0.7349
	G	27.74/0.5859	24.61/0.4254	22.28/0.3190	29.78/0.6369	26.46/0.4862	24.69/0.4017	31.13/0.8544	30.05/0.8094	28.88/0.7484
	B	26.93/0.5688	24.69/0.4110	22.44/0.3058	28.60/0.6213	25.68/0.4748	23.85/0.3913	30.27/0.8373	29.10/0.7910	28.39/0.7295
kodim07	R	26.38/0.5780	23.46/0.4429	21.23/0.3535	29.02/0.6277	26.17/0.5015	24.26/0.4276	30.22/0.8682	29.27/0.8247	28.18/0.7701
	G	26.86/0.5971	23.84/0.4630	21.55/0.3733	29.19/0.6491	25.97/0.5226	24.04/0.4477	30.92/0.8798	30.18/0.8390	28.690.7847
	B	26.12/0.5737	23.23/0.4388	21.09/0.3503	27.80/0.6411	24.93/0.5162	23.06/0.4437	29.22/0.8698	28.40/0.8285	27.60/0.7770
kodim09	R	25.35/0.4686	22.24/0.3282	19.93/0.2454	27.80/0.5252	24.63/0.3888	22.80/0.3143	31.09/0.8590	29.51/0.7680	27.93/0.6805
	G	25.71/0.4822	22.50/0.3411	20.12/0.2565	27.95/0.5371	24.76/0.3996	22.90/0.3240	31.67/0.8619	29.90/0.7699	28.28/0.6815
	B	25.54/0.4636	22.35/0.3234	20.01/0.2398	26.80/0.5175	23.71/0.3800	21.95/0.3040	30.90/0.8543	29.41/0.7630	28.04/0.6762
kodim10	R	25.96/0.5158	22.90/0.3644	20.60/0.2718	28.95/0.5765	25.53/0.4322	23.55/0.3491	31.07/0.8597	29.670.7978	27.99/0.7153
	G	26.32/0.5345	23.15/0.3823	20.81/0.2887	28.73/0.5906	25.43/0.4456	23.42/0.3607	31.75/0.8628	30.21/0.7997	28.47/0.7170
	B	26.07/0.5103	22.97/0.3589	20.67/0.2672	27.79/0.5669	24.72/0.4215	22.86/0.3374	31.09/0.8517	29.76/0.7888	28.24/0.7070
kodim12	R	24.22/0.3854	21.05/0.2536	18.72/0.1797	25.95/0.4278	23.13/0.2913	21.01/0.2233	30.13/0.7788	28.63/0.7148	27.04/0.6444
	G	24.43/0.4000	21.18/0.2656	18.84/0.1910	26.56/0.4475	23.40/0.3106	21.38/0.2406	30.55/0.7907	28.98/0.7295	27.30/0.6609
	B	24.38/0.3869	21.18/0.2557	18.85/0.1819	25.71/0.4424	22.76/0.3057	21.38/0.2367	30.48/0.7805	29.25/0.7188	27.79/0.6508
kodim16	R	26.99/0.6085	24.04/0.4743	21.82/0.3789	29.23/0.6644	26.62/0.5372	24.65/0.4561	31.50/0.8602	30.06/0.8073	28.56/0.7369
	G	27.54/0.6221	24.38/0.4860	22.07/0.3893	29.66/0.6714	26.72/0.5443	24.91/0.4636	32.15/0.8660	30.53/0.8128	29.13/0.7414
	B	26.91/0.6000	24.21/0.4667	21.94/0.3724	28.21/0.6490	25.26/0.5243	23.38/0.4473	30.27/0.8544	29.14/0.8002	27.97/0.7279
kodim20	R	24.29/0.5009	21.32/0.3819	19.07/0.3056	26.78/0.5293	23.57/0.4164	21.23/0.3502	26.96/0.8189	24.47/0.7489	22.39/0.6784
	G	24.61/0.5054	21.59/0.3878	19.32/0.3122	26.44/0.5403	23.50/0.4260	21.33/0.3594	27.52/0.8170	25.01/0.7490	22.93/0.6804
	B	24.84/0.4832	21.98/0.3714	19.76/0.2969	25.86/0.5172	23.28/0.4092	21.50/0.3466	28.46/0.7712	26.67/0.7101	24.89/0.6474
kodim21	R	25.62/0.5777	22.89/0.4619	20.70/0.3815	27.97/0.6358	25.42/0.5201	23.65/0.4489	28.01/0.8356	27.15/0.7863	26.20/0.7300
	G	26.26/0.5902	23.32/0.4737	21.00/0.3929	28.59/0.6373	25.50/0.5230	23.85/0.4534	28.46/0.8433	27.64/0.7950	26.72/0.7411
	B	25.94/0.5716	23.10/0.4552	20.86/0.3744	26.38/0.6137	24.06/0.5023	22.43/0.4347	27.93/0.8157	27.28/0.7671	26.47/0.7122
kodim23	R	26.19/0.5316	23.39/0.3746	21.25/0.2751	28.54/0.5583	25.83/0.4081	24.47/0.3275	30.58/0.8587	29.19/0.8148	27.64/0.7699
	G	26.80/0.5410	23.84/0.3797	21.61/0.2785	28.25/0.5828	25.47/0.4315	23.70/0.3491	32.27/0.8670	31.17/0.8262	29.97/0.7841
	B	26.91/0.5369	23.89/0.3774	21.74/0.2771	27.12/0.5934	25.04/0.4446	24.03/0.3600	31.25/0.8575	30.19/0.8181	29.05/0.7778

4. Conclusions

In this paper, we present a joint denoising and demosaicking algorithm to reconstruct the full color image from noisy CFA data in the blind condition. The proposed algorithm is based on the low rank approximation and color difference model. The experimental results show that our proposed algorithm can achieve higher resolution, less noise and sharper edges. For noisy CFA data, our proposed method not only can remove the noise and the color artifacts effectively, but also can recover rich textures and details. It is also superior to other state-of-the-art methods both quantitatively and qualitatively.

References

[1] Amirgholipour S. and Sharifi A., "A Pre-Filtering Method to Improve Watermark Detection Rate in DCT Based Watermarking," *The International Arab Journal of Information Technology*, vol. 11, no. 2, pp.178-185, 2014.

[2] Buades A., Coll B., and Morel J., "A Review of Image Denoising Algorithms, with a New One," *Multiscale Modeling and Simulation*, vol. 4, no. 2, pp. 490-530, 2005.

[3] Condat L. and Mosaddegh S., "Joint Demosaicking and Denoising by Total Variation Minimization," *in Proceeding of 19th IEEE International Conference on Image Processing (ICIP)*, pp. 2781-2784, 2012.

[4] Gunturk B., Altunbasak Y., and Mersereau R., "Color plane Interpolation Using Alternating Projections," *IEEE Transactions on Image Processing*, vol. 11, no. 9, pp. 997-1013, 2002.

[5] Hirakawa K. and Parks T., "Joint Demosaicking and Denoising," *IEEE Transactions on Image Processing*, vol. 15, no. 8, pp. 2146-2157, 2006.

[6] Li X. and Orchard M., "New Edge-Directed Interpolation," *IEEE Transactions on Image Processing*, vol. 10, no. 10, pp. 1521-1527, 2001.

[7] Menon D. and Calvagno G., "Joint Demosaicking and Denoising with Space-Varying Filters," *IEEE International Conference on Processing (ICIP)*, pp. 477-480, 2009.

[8] Portilla J., Strela V., Wainwright M., and Simoncelli E., "Image Denoising Using Scale Mixtures of Gaussians in the Wavelet Domain," *IEEE Transactions on Image Processing*, vol. 12, no. 11, pp. 1338-1351, 2003.

[9] Rydell J., Knutsson H., and Borga M., "Bilateral Filtering of fMRI Data," *IEEE Journal of Selected Topics in Signal Processing*, vol. 2, no. 6, pp. 891-896, 2008.

[10] Saadi S., Guessoum A., Bettayeb M., and Abdelhafidi K., "Blind Restoration of Radiological Images using Hybrid Swarm Optimized Model Implemented on FPGA," *The International Arab Journal of Information Technology*, vol. 11, no. 5, pp. 476-486, 2014.

[11] Yuk C., Au O., Li R., and Lam S., "Color Demosaicking Using Direction Similarity in Color Difference Spaces," *IEEE International Symposium on Circuits and Systems*, LA, pp. 1281-1284, 2007.

[12] Zhang L., Lukac R., Wu X., and Zhang D., "PCA-Based Spatially Adaptive Denoising of CFA Images for Single-Sensor Digital Cameras," *IEEE Transactions on Image Processing*, vol. 18, no. 4, pp. 797-812, 2009.

[13] Zhang L., Wu X., and Zhang D., "Color Reproduction from Noisy CFA Data of Single Sensor Digital Cameras," *IEEE Transactions on Image Processing*, vol. 16, no. 9, pp. 2184-2197, 2007.

[14] Zhang Y., Ding Y., Liu J., and Guo Z., "Guided Image Filtering Using Signal Subspace Projection," *IET Image Processing*, vol. 7, no. 3, pp. 270-279, 2013.

[15] Zhang Y., Liu J., Li M., and Guo, Z., "Joint Image Denoising Using Aadaptive Principal Component Analysis and Self-Similarity," *Information Sciences*, vol. 259, pp. 128-141, 2014.

[16] Zhang Y., Yang Z., Sun F., and Ai Y., "Improved Color Image Demosaicing with Signal Correlation," *Symposium on Photonics and Optoelectronic*, Chengdu, pp.1-4, 2010.

Xia Zhai received the Bachelor's degree in Art and Design in 2011 from Guangzhou Academy of Fine Arts, P. R. China, and the Master's degree in 2013 from Manchester Metropolitan University, United Kingdom. She is currently a teacher at the Arts Department, Henan University of Economics and Law, P.R. China. Her research interests include digital arts and jewelry art.

Weiwei Guo received the Bachelor's degree in Communication Engineering in 2011 from North China University of Water Resources and Electric Power, P. R. China, and the Master's degree in Information and Communication Engineering in 2014 from University of Electronic Science and Technology of China, P. R. China, respectively. Her research interests include the signal processing and image restoration.

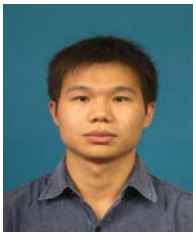

Yongqin Zhang received the B.S.E. degree in Electronics Science and Technology in 2005 from Zhengzhou University, P.R. China, the Ph.D. degree in Communication and Information Systems in 2010 from Wuhan University, P.R. China, respectively. He served as an assistant researcher at Shenzhen Institutes of Advanced Technology, Chinese Academy of Sciences and later as a postdoctoral researcher at the Institute of Computer Science and Technology, Peking University, P.R. China. He is currently a lector at the College of Computer and Information Engineering, Henan University of Economics and Law, P.R. China. His research interests include magnetic resonance imaging, sparse representation and image restoration.

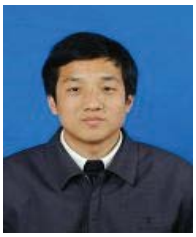

Jinsheng Xiao received the Ph.D. degree in school of mathematics and statistics in 2001 from Wuhan University, Wuhan, P. R. China. He is currently an associate professor at School of Electronic Information, Wuhan University, Wuhan, P.R. China. His current research interests include computer vision, and image/video processing.

Xiaoguang Hu received the Ph.D. degree in Photogrammetry and remote sensing in 2012 from Wuhan University, P.R. China. He is currently a postdoctoral researcher at the College of Engineering, Peking University, P.R. China. His research interests are in biologically-inspired computational vision with technological applications to target detection, and robotics.